HHS Public Access

Neuropeptide Y receptor interactions regulate its mitogenic activity

Magdalena Czarnecka[1], **Congyi Lu**[1,2], **Jennifer Pons**[1], **Induja Maheswaran**[1], **Pawel Ciborowski**[3], **Lihua Zhang**[4], **Amrita Cheema**[4], and **Joanna Kitlinska**[1,5,*]

[1]Department of Physiology and Biophysics, Georgetown University Medical Center, Washington, DC

[2]New York Genome Center, New York, NY, USA

[3]Department of Pharmacology and Experimental Neuroscience, University of Nebraska Medical Center, Omaha, NE, USA

[4]Department of Oncology, Lombardi Comprehensive Cancer Center, Georgetown University Medical Center, Washington, DC, USA

[5]Department of Biochemistry and Molecular & Cellular Biology, Georgetown University Medical Center, Washington, DC, USA

Abstract

Neuropeptide Y (NPY) is a multifunctional neurotransmitter acting via G protein-coupled receptors - Y1R, Y2R and Y5R. NPY activities, such as its proliferative effects, are mediated by multiple receptors, which have the ability to dimerize. However, the role of this receptor interplay in NPY functions remains unclear. The goal of the current study was to identify NPY receptor interactions, focusing on the ligand-binding fraction, and determine their impact on the mitogenic activity of the peptide. Y1R, Y2R and Y5R expressed in CHO-K1 cells formed homodimers detectable on the cell surface by cross-linking. Moreover, Y1R and Y5R heterodimerized, while no Y2R/Y5R heterodimers were detected. Nevertheless, Y5R failed to block internalization of its cognate receptor in both Y1R/Y5R and Y2R/Y5R transfectants, indicating Y5R transactivation upon stimulation of the co-expressed receptor. These receptor interactions correlated with an augmented mitogenic response to NPY. In Y1R/Y5R and Y2R/Y5R transfectants, the proliferative response started at picomolar NPY concentrations, while nanomolar concentrations were needed to trigger proliferation in cells transfected with single receptors. Thus, our data identify direct and

indirect heterotypic NPY receptor interactions as the mechanism amplifying its activity. Understanding these processes is crucial for the design of treatments targeting the NPY system.

Keywords

Neuropeptide Y; G protein-coupled receptors; homodimerization; heterodimerization; proliferation

Introduction

Neuropeptide Y (NPY) is a 36-amino acid sympathetic neurotransmitter abundant in the central and peripheral nervous systems (1). While the peptide is mainly known as a regulator of various physiological functions, such as stress response, food intake and blood pressure, there is also growing evidence of its growth-promoting activities (2–13). NPY stimulates proliferation in a variety of cell types, including vascular, neuronal and tumor cells, contributing to tissue regeneration and growth-related pathologies (14–22).

NPY actions are mediated by multiple G-protein coupled receptors (GPCRs), consisting of seven transmembrane helices connected by three intracellular loops and two terminal domains (23). The extracellular N-terminal domain of GPCRs is commonly glycosylated, while intracellular domains undergo other post-translational modifications, such as phosphorylation (24, 25). These secondary changes regulate various receptor functions, including protein folding, activity, trafficking, localization and cell-cell interactions.

NPY receptors expressed in humans encompass Y1R, Y2R and Y5R, while Y4R predominantly binds another peptide from the NPY family, pancreatic polypeptide (PP) (23, 26). These receptors act mainly via pertussis toxin-sensitive $G_{i/o}$ proteins triggering the decrease in 3',5'-cyclic adenosine monophosphate (cAMP) synthesis and mobilization of intracellular calcium (27–29). The mitogenic effects of NPY are mediated by p44/42 mitogen-activated protein kinase (MAPK) (20, 29–33). While each of the NPY receptors has been assigned its own unique functions, there is also growing evidence of their interactions. For example, Y1R and Y5R are frequently co-localized in the brain and have been implicated in the same physiological processes, e.g. regulation of food intake (34–36). Moreover, expression of multiple NPY receptors has been associated with amplification of its proliferative functions, manifested by the presence of an additional peak of mitogenic activity at picomolar concentrations, which are below known affinities for single NPY receptors (29, 37). This high-affinity response was observed in a variety of cells proliferating upon NPY stimulation, including vascular smooth muscle, endothelial and tumor cells, suggesting the universal nature of this phenomenon (29, 31, 37, 38). Nevertheless, the role of NPY receptor interactions in augmenting its effects has not been directly proven.

The potential role of NPY receptor interactions in regulation of NPY functions has been supported by dimerization of the NPY receptors. All NPY receptor types have been shown to form homodimers, while some studies suggest heterodimerization of Y1R and Y5R (39–47). However, the functional role of such receptor interactions remains elusive and the data pertaining to the pharmacological changes and receptor behavior upon ligand stimulation vary depending on methodology and experimental design. Importantly, most previous

studies analyzed the entire receptor population within the cell, including intracellular fraction, which is not involved in ligand binding (39–47). In addition, experiments with bivalent receptor ligands did not support the postulated role of receptor dimerization in augmenting NPY functions (48, 49). Thus, the goal of the current study was to characterize NPY receptor interactions with the focus on their ligand-binding fraction present on the plasma membrane and determine the impact of these processes on peptide functions. Using mitogenic activity of NPY as a model, we provided direct evidence for a crucial role of heterotypic receptor interactions in enhancing actions of the peptide.

Materials and Methods:

Materials

NPY was purchased from Bachem (San Carlos, CA). Y5R agonist, BWX 46, and Y5R antagonist, CGP71683, were obtained from Tocris (Ellisville, MO). Y1R agonist, [Arg6, Pro34]NPY, and Y2R agonist, [ahx(5-24)]NPY, were provided by Dr. Annette Beck-Sickinger, University of Leipzig, Germany.

Cell culture

CHO-K1 cells were obtained from American Type Culture Collection (Manassas, VA) and cultured in F12K media supplemented with 10% fetal bovine serum (FBS), according to the supplier's recommendation.

Cloning and transfection

cDNAs of human Y1R, Y2R, and Y5R were cloned into pEGFP-N1 vector at NheI and BamHI restriction sites. Puromycin resistance and mCherry tag was acquired by subcloning NPY receptor-EGFP fusion protein into pIRESpuro3 vector using NheI and NotI restriction enzymes and replacing EGFP tag with mCherry from pmCherry-N1 vector, using BamHI and NotI restriction sites. All vectors were obtained from Clontech Laboratories (Mountain View, CA) and restriction enzymes from New England BioLabs (Ipswich, MA). The presence of NPY receptor and fluorescent protein sequences in the vector constructs was confirmed by restriction analysis and sequencing. Transfection of CHO-K1 was performed using Lipofectamine 2000 (Invitrogen, Carlsbad, CA). Stable transfectants carrying EGFP-fused NPY receptors were selected with geneticin (Sigma, St. Louis, MO) at a concentration of 1mg/ml followed by the single cell clone isolation. To obtain cells expressing Y1R/Y5R and Y2R/Y5R, CHO-K1/Y5REGFP stable transfectants were co-transfected with pIRESpuro3/Y1R-mCherry or pIRESpuro3/Y2-mCherry vectors and stable double transfectants selected with geneticin and puromycin (Sigma, St. Louis, MO) at concentrations of 1mg/ml and 0.5 mg/ml, respectively. The selection was followed by single cell clone isolation. Clones with high membrane NPY receptor expression were selected for further analyses.

p44/42 signaling

Stable transfectants were treated with NPY or selective NPY receptor agonists at 10^{-7}M for the desired time (1–90min). The cells were lysed immediately after treatment. Total and phosphorylated p44/42 MAPK were detected in the cell lysates using the following

antibodies: mouse monoclonal anti-phospho p44/42 E10 and anti-p44/42 MAPK (Cell Signaling, Danvers, MA, USA). The band intensities were quantified by densitometry using ImageJ software.

Cyclic AMP assay

Stable transfectants were primed with 10 μM phosphodiesterase inhibitor, 3-Isobutyl-1-methylxanthine (IBMX), for 1 hour and then treated with 10μM forskolin, an adenylyl cyclase activator, and with the desired NPY receptor ligand at a concentration of 10^{-7}M for 1 hour. The levels of intracellular cAMP were measured using cAMP Biotrak Enzymeimmunoassay (EIA) System (GE Healthcare, Pittsburgh, PA), according to the manufacturer's instructions.

Western blot analysis of NPY receptor homodimers

CHO-K1 cells stably transfected with EGFP-fused NPY receptors were treated with 10^{-7}M NPY for 15 minutes followed by crosslinking with membrane-impermeable bis[sulfosuccinimidyl] suberate (BS3) at concentration 0.5 mM for 30 minutes. Western blot for NPY receptors was performed on membrane proteins isolated as previously described, using rabbit polyclonal anti-EGFP antibody (Clontech, Mountain View, CA) (30, 32, 50). To elucidate glycosylation pattern of the NPY receptors, cell membrane fractions were deglycosylated with PNGase F (Sigma, St. Louis, MO) prior to Western blotting, according to the manufacturer's protocol.

Mass spectrometry

CHO-K1/Y5R-EGFP cells, with or without BS3 pre-treatment, were lysed and the receptors were pulled down using Pierce Classic Immunoprecipitation (IP) Kit (Thermo Scientific, Waltham, MA) and rabbit anti-EGFP Ab (Clontech, Mountain View, CA). IP eluates were separated on SDS-PAGE Tris-Glycine gel and stained with Coomassie Brilliant Blue dye. Gels were dehydrated and fixed. The position of the Y5R-rich bands was determined by performing the Western Blot on one part of the gel, and comparing the results of blotting for Y5R with the second part of a gel stained with Coomassie Blue. Bands corresponding to the monomers, and higher order complexes of Y5R were excised from the gel and subjected to in-gel tryptic digest followed by nanoLC-MS/MS analysis performed at Georgetown University Proteomics & Metabolomics Shared Resource.

Immunoprecipitation and Western blot analysis of NPY receptor heterodimers

CHO-K1 cells transfected with two NPY receptors (Y1R/Y5R or Y2R/Y5R) were treated with 10^{-7}M NPY for 10 minutes, with or without 15 min pre-treatment with Y5R antagonist at concentration 10^{-6}M, followed by crosslinking with 0.5mM BS3 for 30 minutes. The cells were lysed in the buffer containing 50mM Tris HCl, pH 7, 150mM NaCl, protease inhibitors cocktail, 1mM IGEPAL CA 630 and 10mM iodoacetamide (all reagents obtained from Sigma, St. Louis, MO). Immunoprecipitation was performed using Pierce Classic IP Kit (Thermo Scientific, Waltham, MA) and goat anti-Y5R antibody (Everest Biotech, Oxfordshire, UK). Receptor complexes were detected by Western blotting using anti-dsRed

or anti-GFP antibodies (Clontech, Mountain View, CA) to detect Y1R-mCherry and Y2R-mCherry or Y5R-EGFP fusion proteins, respectively.

Live cell imaging analysis of NPY receptor internalization

Nikon Eclipse TE-300 Spinning Disk Timelapse Microscope System was used for receptor trafficking experiments. Transfectants were plated in LabTek II 8-well chamber system at a density of 12,000 cells per well and treated with NPY (10^{-7}M), with or without 15 min pre-treatment with Y5R antagonist (10^{-6}M). Readings were collected up to 30 minutes for at least 6 cells per treatment group. The NPY-induced changes in fluorescence intensity of NPY receptors fused to EGFP or mCherry in different subcellular regions were measured using ImageJ software. The measurements were performed on slices of grayscale images at the same position within z-stacks at different time points for each receptor separately. The regions with membrane expression of the given receptors were selected at the start of the experiment, before NPY treatment. Within these regions, membrane areas and adjacent intracellular areas were identified. The ratio of membrane to cytoplasm mean fluorescence intensities (membrane/cytosol) was calculated for each region to reflect the degree of accumulation of receptors on the cell membrane. The regions with the membrane to cytoplasm ratio above 1.0 at the beginning of the experiment were considered as having membrane receptor expression and selected for further analyses. The NPY-induced changes in membrane/cytosol ratios were calculated at each time point. Additionally, for each treatment, a representative region was selected to visualize changes in the receptor distribution, based on fluorescence intensity along the line crossing the cell membrane in the selected region. Multiple regions from at least 5 cells per treatment were included in the analysis.

Cell growth assay

Cells plated in 96-well plates were cultured in 1% FBS media for 24h and treated as desired. After 24h, the number of viable cells was assessed using MTS-based CellTiter 96®AQueous One Solution Cell Proliferation Assay (Promega, Madison, WI). Additionally, 3H-thymidine uptake was performed to confirm the mitogenic effect of NPY, as previously described (16, 29, 38).

Bioinformatics analysis

Human NPY receptor sequences were obtained from the Universal Protein Resource (UniProt) database entries: P25929 (Y1R), P49146 (Y2R), Q15761 (Y5R), and analyzed for the presence of putative glycosylation sites.

Statistical analyses

Statistical analyses were performed using SigmaStat® or GraphPad software. Between-group comparisons were assessed using one-way repeated measures ANOVA with post-hoc t-test, independent-samples t-tests or paired-samples t-tests, as appropriate. For analysis of the receptor internalization by time-lapse microscopy, paired t-test was utilized. Significant associations were assessed at an alpha level of 0.05. All experiments were repeated at least three times. Data is presented as mean ± standard errors.

Results:

NPY receptors fused to fluorescent proteins preserve their functionality.

To create experimental tools suitable to investigate NPY receptor interactions, we used CHO-K1 cells lacking endogenous expression of NPY and its receptors. The cells were stably transfected with vectors encoding human NPY receptors fused to fluorescent proteins, either EGFP or mCherry via the intracellular C-terminus of the receptors to prevent interference with ligand binding. In contrast to fluorescent proteins alone that are localized mainly in the nucleus and cytoplasm, NPY receptors fused to these proteins were present in the plasma membrane and intracellular vesicles, in agreement with their natural subcellular localization (Fig. 1A). Importantly, NPY receptors that were fused to fluorescent proteins preserved their activity, as shown by NPY-induced transient MAPK activation and decreased cAMP levels previously described for these receptors in native cells (Fig. 1B–D).

NPY receptors vary in their glycosylation pattern and ability to form homodimers.

Western blot analysis of NPY receptors stably expressed in CHO-K1 cells revealed the presence of their multiple forms. Y1R-EGFP protein was detectable as two bands at apparent molecular weights of approximately 80 and 100 kDa, which is higher than the weight predicted based on the amino acid sequence (71 kDa) (Fig. 2A). The localization of these bands did not change upon NPY treatment. However, when CHO-K1/Y1R-EGFP cells were treated with NPY followed by membrane non-permeable cross-linker, BS3, the higher order complex below 200 kDa became detectable. The deglycosylation of the cell lysates from CHO-K1/Y1R-EGFP transfectants resulted in a significant shift of the band motility (Fig. 2A). Upon PNGase F treatment, two bands that were detectable in untreated cells converted into one band of approximately 70 kDa, corresponding to the predicted molecular weight of the monomeric Y1R-EGFP, based on the amino acid sequence. This result suggested the presence of differentially glycosylated Y1R monomers. In lysates from cells treated with NPY and BS3, two bands remained detectable upon deglycosylation - 70kDa corresponding to the deglycosylated monomer and the higher band of approximately140 kDa (Fig. 2A). The two-fold difference in molecular weight between the monomer and the high order band, and their similar mobility shift upon deglycosylation indicated that the higher band represented the Y1R homodimer that consists of glycosylated forms of the receptor. This profound shift in electrophoretic mobility and the existence of differentially glycosylated forms of Y1R is in agreement with the presence of three putative N-glycosylation sites within the N-terminus of the receptor, based on UniProt analysis (Fig. 2D).

The Y2R-EGFP fusion protein was detectable as one distinct band at the apparent molecular weight of approximately 85 kDa (Fig 2B). Treatment with BS3 cross-linker revealed the presence of high molecular weight bands below 200 kDa, independently of NPY treatment. Deglycosylation of the CHO-K1/Y2R-EGFP lysates led to a slight shift in electrophoretic mobility of low and high molecular weight bands, suggesting the presence of the receptor monomer with low level of glycosylation and the homodimer, the formation of which did not depend on ligand stimulation. The modest shift in band motility upon deglycosylation and

lack of differentially glycosylated forms of the receptor is in line with the presence of a single putative N-glycosylation site in the Y2R amino acid sequence (Fig. 2D).

Similar to Y1R, Y5R presented as two bands with apparent molecular weights of 90 and 100 kDa (Fig. 2C). The PNGase F treatment converted these two bands into one with electrophoretic mobility corresponding to the molecular weight predicted by the amino acid sequence (78kDa), confirming that they represent differentially glycosylated receptor monomers. Consistent with this observation, UniProt analysis revealed the presence of two putative N-glycosylation sites within the Y5R amino acid sequence (Fig. 2D). Interestingly, in CHO-K1/Y5R-EGFP lysates, high molecular weight forms corresponding to putative homodimers were detectable independently of the ligand treatment, even in the absence of the cross-linker (Fig. 2C). The ability of the oligomeric Y5R forms to withstand denaturing and reducing conditions of the SDS-PAGE gel was further confirmed by immunoprecipitation with anti-GFP antibody, which facilitated detection of these complexes in cells not treated with BS3 (Fig. 2C). In contrast to Y1R and Y2R oligomers, the high molecular weight band of Y5R did not shift upon PNGase F treatment. Nevertheless, Mass spectrometry analysis of these bands detectable in immunoprecipitated samples confirmed the presence of Y5R.

Co-expression of Y1R and Y5R leads to formation of heterodimers.

To mimic interactions between heterotypic NPY receptors implicated in various physiological and pathological conditions, CHO-K1 cells were stably transfected with two different NPY receptors fused to various fluorescent proteins. CHO-K1/Y1R-mCherry/Y5R-EGFP cells (Y1R/Y5R transfectants) expressed both receptors in their monomeric forms (Fig. 3A). Importantly, both Y1R and Y5R preserved the glycosylation patterns observed for single receptor transfectants, as evidenced by the presence of two distinct forms with molecular weights exceeding those predicted by amino acid sequences (Fig. 3A, Fig. 2A, C). These receptors were functional and responsive to their selective agonists, as evidenced by MAPK activation (Fig. 3B). Microscopic images of established transfectants revealed co-localization of the Y1R and Y5R on the cell membrane and in intracellular vesicles (Fig 3C).

To determine if the Y1R/Y5R co-localization results from their direct interactions and formation of heterodimers, Y1R/Y5R transfectants were treated with membrane impermeable cross-linker, BS3, and then the resulting lysates were subjected to immunoprecipitation with anti-Y5R antibody. The immunoprecipitates were then immunoblotted with anti-GFP and anti-dsRed antibody to detect Y5R-EGFP and Y1R-mCherry fusion proteins, respectively. Western blot confirmed the presence of Y5R-EGFP protein in the immunoprecipitates, detectable as two monomeric forms (Fig. 3D). Moreover, in BS3-treated cells, a high molecular weight form of Y5R with an apparent molecular weight exceeding 170 kDa was observed. Importantly, Western blot with anti-dsRed antibody revealed co-immunoprecipitation of the Y1R-mCherry detectable at the same >170 kDa band, implicating the presence of Y1R/Y5R heterodimers on the cell surface. No such band was detected in control samples without BS3. In contrast to the increase in putative Y1R homodimer content observed in Y1R single transfectants upon NPY treatment (Fig.

2A), Y1R content in high molecular weight Y1R/Y5R complexes were detectable without NPY and decreased upon ligand stimulation, as evidenced by reduced Y1R content at the >170 kDa band (Fig. 3D–E). This effect was not prevented by Y5R antagonist. The remaining Y5R detectable at the high molecular band of lysates from NPY- and BS3-treated Y1R/Y5R transfectants may represent Y5R homodimers that are detectable in the single transfectants as well (Fig. 2C, Fig. 3D).

Interactions between Y1R and Y5R change their internalization pattern.

Internalization of GPCRs may serve as a measure of their responsiveness to ligand stimulation. To determine if NPY receptor interactions change their internalization pattern, we measured their trafficking upon ligand stimulation. In CHO-K1/Y5R-EGFP cells, NPY treatment resulted in rapid Y5R internalization in regions of its initial membrane localization (Fig. 4A). The decrease in the membrane fraction of the receptor was detectable 7 min upon NPY administration, and further enhanced at 17 min. The NPY-induced Y5R internalization was prevented by Y5R antagonist (Fig. 4B).

In CHO-K1 cells stably transfected with Y1R-mCherry and Y5R-EGFP, NPY triggered internalization of both receptors in areas of their initial membrane localization (Fig. 5A). However, unlike in CHO-K1/Y5R-EGFP cells, Y5R antagonist delayed the internalization of Y1R and Y5R, but did not block it, as manifested by the significant decrease in the membrane fraction of the receptors detectable 17 min after NPY administration (Fig. 5B). This change in Y5R internalization pattern confirmed Y1R/Y5R interactions suggested by the crosslinking experiment above.

Y2R and Y5R interact with each other despite the lack of direct binding.

To test Y2R/Y5R interactions we used CHO-K1 cells stably transfected with both receptors fused to mCherry and EGFP, respectively (CHO-K1/Y2R-mCherry/Y5R-EGFP cells) (Fig. 6A). Both receptors preserved their activity, as indicated by p44/42 MAPK activation upon stimulation with selective receptor agonists (Fig. 6B). Similar to Y1R, Y2R co-localized with Y5R on the membrane and in intracellular vesicles of these cells (Fig. 6C). However, a crosslinking experiment followed by immunoprecipitation with anti-Y5R and Western blot with anti-dsRed antibody revealed no Y2R-mCherry fusion protein in the molecular weight range corresponding to monomers or dimers, indicating a lack of direct heterodimerization of these receptors (data not shown). Despite that, however, microscopic analysis of the receptor trafficking demonstrated significant changes in Y5R internalization in the CHO-K1/Y2R-mCherry/Y5R-EGFP cells, as compared to those transfected with single Y5R-EGFP. Upon NPY stimulation, Y2R and Y5R simultaneously internalized in regions of their initial membrane localization, with receptor internalization observed at 14 min (Fig. 7A). However, pre-treatment with Y5R antagonist did not block Y5R internalization. Y2R and Y5R rapidly internalized upon NPY stimulation (4 min) (Fig. 7B). However, at 14 min post-treatment, Y5R remained intracellular, while Y2R recycled back to the membrane.

Co-expression of NPY receptors changes the proliferative response of the cells.

Previous data indicate that interactions between NPY receptors increase their sensitivity to NPY stimulation, resulting in a mitogenic response to picomolar concentrations of the

peptide, often in a characteristic bimodal manner (16, 29, 31, 37, 38). To directly test this hypothesis, we used CHO-K1 cells transfected with single and double NPY receptors and measured the growth response to peptide stimulation using MTS assay, which allows for the detection of changes in proliferation and cell death. Thymidine uptake was used to confirm increased cell proliferation in CHO-K1 transfectants responding to NPY with augmented growth. In line with a lack of endogenous NPY receptors in CHO-K1 cells, no proliferative response was observed in nontransfected cells and those stably expressing EGFP alone (Fig. 8A). In contrast, a profound mitogenic effect of NPY was detected by MTS assay and thymidine uptake in cells transfected with Y1R-EGFP and Y2R-EGFP, starting at a 10^{-8}M concentration of NPY (Fig. 8A). No such response was observed in the CHO-K1/Y5R-EGFP cells. The pattern of this mitogenic effect changed in cells transfected with two NPY receptors. In the Y2R-mCherry/Y5R-EGFP transfectants we observed a characteristic bimodal proliferative response, with two peaks of activity at low (10^{-13}M) and high (10^{-7}M) NPY concentrations (Fig. 8B). Similarly, proliferative activity of NPY at picomolar concentrations was detected in some Y1R-mCherry/Y5R-EGFP clones, while in others NPY exerted a bimodal growth-inhibitory effect (Fig. 8C). CHOK1/Y1R-mCherry/Y5R-EGFP clones that exhibited a growth-inhibitory response to NPY had lower Y1R levels and thereby reduced ratio of Y1R/Y5R activity measured by decreases in cAMP concentrations upon Y1R and Y5R agonist stimulation, as compared to cells proliferating in response to NPY (Fig. 8D–E).

Discussion

Despite growing evidence for GPCR homo- and heterodimerization, the functional outcomes of these interactions remain elusive. Within the NPY receptor family, all receptors have been shown to form homodimers, while Y1R additionally can heterodimerize with Y5R, Y4R and β-adrenergic receptors (39–47). Nevertheless, reports pertaining to the receptor fate upon agonist stimulation vary depending on the methodology, while experiments with bivalent ligands do not support their enhanced ability to stimulate NPY receptors (48, 49). Thus, the goal of the current study was to characterize NPY receptor interactions in live cells, as well as the impact of these processes on the receptor activation and function. In contrast to previous studies using fluorescence and bioluminescence resonance energy transfer methods (FRET and BRET, respectively), as well as isolated membrane preparations, all of which analyzed the entire population of the receptors present in the cells, we have focused on their active fraction present on the plasma membrane and responsible for ligand binding (39–47). To elucidate the functional role of the receptor interactions, we used the mitogenic activity of NPY as a model, since previous results from our laboratory strongly implicated the role for the heterotypic NPY receptor expression in augmenting its growth-regulatory effects in various cells (29, 37). However, our findings may also pertain to other NPY functions mediated by multiple receptors, such as central regulation of food intake, anxiolytic effects and others (23, 34, 51).

Using membrane non-permeable cross-linker, BS3, we confirmed the presence of high molecular weight bands for Y1R, Y2R and Y5R on the surface of CHO-K1 stable transfectants. As these bands correspond to double the molecular weight of monomers detected in these cells, they most likely represent receptor homodimers previously reported

by other groups (39, 40, 42–46). This method has previously been utilized to demonstrate the presence of Y4R homodimers (39). Moreover, such high molecular weight bands were previously observed for native Y1R in the cell membrane fraction obtained from brain tissue, validating our findings in transfected cells (36). Interestingly, in our study, Y1R homodimers were detectable only in the presence of NPY, while Y2R and Y5R homodimers were ligand-independent. In contrast, previous FRET studies performed on entire cells indicated no change in homodimerization upon agonist stimulation, while density gradient studies indicated their ligand-induced disassociation (39, 40, 43, 46). These discrepancies may result from methodological differences. In our study, we focused on the extracellular domain of receptors present on the plasma membrane, while FRET studies were based on the interactions of fluorescent proteins fused to their intracellular domain and tested the entire receptor population (40). Therefore, in the case of Y1R, NPY binding may trigger conformational changes in the N-terminus of the receptor, allowing for cross-linking to occur. On the other hand, although the density gradient experiments strongly indicate homodimer disassociation upon stimulation, they do not take into consideration the potential reoligomerization and recycling of the receptors that may occur in live cells (43, 46). Of all homodimers detected, Y5R dimers appeared to be the most stable, as they were detectable without a cross-linker under reducing conditions. These data suggest the possibility of a covalent binding between Y5Rs.

In addition to NPY receptor interactions, our studies revealed also their frequent post-translational modifications. All three NPY receptors were glycosylated, with Y1R and Y5R presenting as differentially glycosylated forms. The presence of differentially glycosylated forms of the native Y1R and Y5R was previously implicated by the presence of double bands migrating slightly higher than the predicted molecular weight for monomers in the membrane fractions from neuronal and tumor tissue (36, 52, 53). This observation is in agreement with the presence of multiple N-glycosylation sites in these two receptors. Interestingly, the presence of the glycosylated forms in oligomers varied between the receptors. The Y1R and Y2R high molecular weight bands shifted upon deglycosylation, indicating that this oligomeric form is comprised of the glycosylated forms of these receptors and further proving that they indeed represent receptor homodimers. In contrast, the high molecular band form of Y5R remained unchanged upon deglycosylation, despite a profound shift in the migration of the monomeric forms, suggesting that the putative homodimer consists of the receptors lacking extensive glycosylation. Altogether, these observations indicate that NPY receptor glycosylation may modify their ability to interact and dimerize. Further studies are required to determine the role of these processes in the regulation of NPY receptor functions.

In addition to its ability to form stable homodimers, Y5R also formed heterodimers with Y1R. Both receptors co-localized on the surface of the CHO-K1/Y1R-mCherry/Y5R-EGFP transfectants. The cross-linking studies confirmed the presence of the Y1R/Y5R heterodimers. The heterodimer content on the cell surface decreased upon NPY treatment. In contrast, previous studies performed by FRET on whole cells indicated no effect of non-selective ligand binding on Y1R/Y5R heterodimerization (41). Thus, the decrease in heterodimer content on the cell surface observed in our study may reflect receptor internalization upon stimulation, rather than their disassociation. This hypothesis was

confirmed by live cell microscopy that revealed coordinated internalization of both receptors after NPY treatment. Importantly, cross-linking and microscopy studies indicated that Y5R internalization was not prevented by Y5R antagonist alone in CHOK1/Y1R-mCherry/Y5R-EGFP cells, while the same compound was fully effective in cells expressing only Y5R. These results indicate that stimulation of Y1R alone is sufficient to activate the heterodimer, as suggested by previous studies (41, 47). This effect may result from the transactivation of Y5R by the stimulated Y1R and can explain amplification of the NPY signal in cells expressing both receptors (Fig. 9). If single receptor occupancy is also sufficient to activate NPY receptor homodimers, this phenomenon may explain the lack of enhanced receptor activation by bivalent ligands (48, 49).

In contrast to Y1R/Y5R interactions, Y2R and Y5R did not form heterodimers detectable by cross-linking, as indicated by previous studies (41, 47). Despite that, however, the receptors strongly co-localized on the cell surface and their internalization pattern was altered, as compared to Y5R alone. Y2R and Y5R internalized simultaneously immediately upon NPY treatment, and Y5R antagonist did not prevent Y5R internalization, like in cells expressing Y1R and Y5R. However, at the later time points, Y5R remained intracellular in the presence of Y5R antagonist, while Y2R recycled back to the cell membrane. These data suggest that despite the lack of direct binding between Y2R and Y5R, these receptors interact with each other, possibly as a part of a larger protein complex (Fig. 9). As in the case of the Y1R/Y5R heterodimers, stimulation of Y2R alone was sufficient to internalize and therefore activate both receptors, suggesting Y5R transactivation again. This phenomenon has been previously described for TrkB and Y5R, which also did not form dimers detectable by cross-linking (30).

The above findings were confirmed by the pattern of mitogenic response to NPY in CHO-K1 cells transfected with single or multiple NPY receptors. Cells expressing Y1R or Y2R alone responded only to nanomolar NPY concentrations, while co-expression of Y5R in these cells triggered the proliferative effect at picomolar concentrations of the peptide. Remarkably, such a high-affinity mitogenic effect of NPY was previously reported in native cells expressing multiple receptors – vascular smooth muscle cells expressing Y1R and Y5R, as well as endothelial and neuroblastoma cells where NPY-induced proliferation is mediated by Y2R and Y5R (29, 31, 37, 38). In all of these cell types, the presence of both receptor antagonists was required to block the high affinity mitogenic response, which is in line with our data on receptor internalization suggesting that single receptor occupancy is sufficient to trigger a signal from both Y1R/Y5R and Y2R/Y5R complexes (Fig. 9) (29, 31, 37, 38). Altogether, these results indicate that independent of the nature of NPY receptor interactions, their heterotypic expression provides the amplification mechanisms at low agonist concentrations.

In the majority of the double-transfectant clones tested in our study, activity of Y1R or Y2R significantly exceeded that of Y5R, which is also observed in native cells, as Y5R is often an inducible receptor (30, 31). As described above, this expression pattern was associated with an enhanced proliferative effect. Interestingly, however, in cells expressing relatively high levels of Y5R (Y1R/Y5R activity ratio below 2) NPY exerted bimodal growth-inhibitory effects. Such an effect was previously described in Ewing sarcoma cells that constitutively

express Y1R, along with unusually high endogenous Y5R levels due to the stimulatory effect of the oncogenic fusion protein – EWS-FLI1 (31, 54). In these cells, unlike in the majority of other cellular models, NPY acting via Y1R and Y5R-stimulated cell death mediated by poly(ADP-ribose) polymerase (PARP-1) and apoptosis-inducing factor (AIF) (55). Therefore, the actions of NPY are regulated not only by the presence of its multiple receptors, but also by their ratio, possibly by forming higher order complexes with altered signaling. Further studies are necessary to determine if the growth-inhibitory effect of NPY in CHO-K1 transfectants is mediated by the same cell death pathways as in Ewing sarcoma and identify the exact molecular mechanisms enabling this switch in NPY actions.

In summary, the activation of NPY receptor monomers and/or homodimers is sufficient to mediate functions of the peptide at its high concentrations, while the response to low levels of NPY is facilitated by heterotypic interactions of receptors. Such synergy may depend on either receptor heterodimerization, as shown for Y1R/Y5R, or indirect interactions demonstrated for Y2R and Y5R. In both cases, activation of a single receptor leads to transactivation of the other NPY receptor in the complex, enhancing the signal from one ligand molecule. Unlike in the case of homodimers, this signal may be further amplified by a signaling cross-talk between pathways activated by heterotypic NPY receptors (Fig. 9). Further studies are required to determine the detailed mechanisms underlying these processes and the role of posttranslational modifications in the receptor functions. Understanding of these complex receptor interactions will provide a rationale for better therapeutic strategies designed to either enhance the beneficial effects of the peptide or inhibit its pathological actions. Thus far, despite multifaceted actions of NPY and its crucial role in processes underlying a variety of disorders, the use of NPY receptors as therapeutic targets has proven to be challenging, largely due to the complexity of the system (3, 5–9, 12, 56, 57). Our data strongly indicate that targeting multiple NPY receptors may be a more effective therapeutic strategy.

Acknowledgements

Nonstandard abbreviations

AIF	apoptosis-inducing factor
BS3	bis[sulfosuccinimidyl] suberate
BRET	bioluminescence resonance energy transfer
CHO-K1	Chinese hamster ovary cells, sub-clone K1
EGFP	Enhanced Green Fluorescent Protein

EWS-FLI1	Ewing sarcoma breakpoint region 1 and friend leukemia integration 1 transcription factor fusion
FRET	fluorescence resonance energy transfer
GPCR	G protein-coupled receptor
IBMX	3-Isobutyl-1-methylxanthine
IP	Immunoprecipitation
MAPK	mitogen-activated protein kinase
MTS	3-(4,5-dimethylthiazol-2-yl)-5-(3-carboxymethoxyphenyl)-2-(4-sulfophenyl)-2H-tetrazolium, inner salt
nanoLC-MS/MS	nanoscale liquid chromatography coupled to tandem mass spectrometry
NPY	neuropeptide Y
PARP-1	poly(ADP-ribose) polymerase
PNGase F	Peptide-N-Glycosidase F
TrkB	tropomyosin receptor kinase A
UniProt	Universal Protein Resource
Y1R	neuropeptide Y receptor type 1
Y2R	neuropeptide Y receptor type 2
Y4R	neuropeptide Y receptor type 4
Y5R	neuropeptide Y receptor type 5

References:

1. Tatemoto K, Carlquist M, and Mutt V (1982) Neuropeptide Y--a novel brain peptide with structural similarities to peptide YY and pancreatic polypeptide. Nature 296, 659–660 [PubMed: 6896083]

2. Zukowska-Grojec Z (1995) Neuropeptide Y. A novel sympathetic stress hormone and more. Ann N Y Acad Sci 771, 219–233 [PubMed: 8597401]

3. Zhang L, Bijker MS, and Herzog H (2011) The neuropeptide Y system: pathophysiological and therapeutic implications in obesity and cancer. Pharmacol Ther 131, 91–113 [PubMed: 21439311]

4. Zukowska Z, Pons J, Lee EW, and Li L (2003) Neuropeptide Y: a new mediator linking sympathetic nerves, blood vessels and immune system? Can J Physiol Pharmacol 81, 89–94 [PubMed: 12710520]

5. Duarte-Neves J, Pereira de Almeida L, and Cavadas C (2016) Neuropeptide Y (NPY) as a therapeutic target for neurodegenerative diseases. Neurobiol Dis 95, 210–224 [PubMed: 27461050]

6. Kautz M, Charney DS, and Murrough JW (2017) Neuropeptide Y, resilience, and PTSD therapeutics. Neurosci Lett 649, 164–169 [PubMed: 27913193]

7. Peng S, Zhou YL, Song ZY, and Lin S (2018) Effects of Neuropeptide Y on Stem Cells and Their Potential Applications in Disease Therapy. Stem Cells Int 2017, 6823917

8. Rodriguez FD, and Covenas R (2017) Targeting NPY, CRF/UCNs and NPS Neuropeptide Systems to Treat Alcohol Use Disorder (AUD). Current medicinal chemistry 24, 2528–2558 [PubMed: 28302012]

9. Yi M, Li H, Wu Z, Yan J, Liu Q, Ou C, and Chen M (2017) A Promising Therapeutic Target for Metabolic Diseases: Neuropeptide Y Receptors in Humans. Cell Physiol Biochem 45, 88–107 [PubMed: 29310113]

10. Heilig M (2004) The NPY system in stress, anxiety and depression. Neuropeptides 38, 213–224 [PubMed: 15337373]

11. Lee NJ, and Herzog H (2009) NPY regulation of bone remodelling. Neuropeptides 43, 457–463 [PubMed: 19748118]

12. Reichmann F, and Holzer P (2016) Neuropeptide Y: A stressful review. Neuropeptides 55, 99–109 [PubMed: 26441327]

13. Tasan RO, Verma D, Wood J, Lach G, Hormer B, de Lima TC, Herzog H, and Sperk G (2016) The role of Neuropeptide Y in fear conditioning and extinction. Neuropeptides 55, 111–126 [PubMed: 26444585]

14. Kuo LE, Kitlinska JB, Tilan JU, Li L, Baker SB, Johnson MD, Lee EW, Burnett MS, Fricke ST, Kvetnansky R, Herzog H, and Zukowska Z (2007) Neuropeptide Y acts directly in the periphery on fat tissue and mediates stress-induced obesity and metabolic syndrome. Nat Med 13, 803–811 [PubMed: 17603492]

15. Lee EW, Michalkiewicz M, Kitlinska J, Kalezic I, Switalska H, Yoo P, Sangkharat A, Ji H, Li L, Michalkiewicz T, Ljubisavljevic M, Johansson H, Grant DS, and Zukowska Z (2003) Neuropeptide Y induces ischemic angiogenesis and restores function of ischemic skeletal muscles. J Clin Invest 111, 1853–1862 [PubMed: 12813021]

16. Pons J, Kitlinska J, Ji H, Lee EW, and Zukowska Z (2003) Mitogenic actions of neuropeptide Y in vascular smooth muscle cells: synergetic interactions with the beta-adrenergic system. Can J Physiol Pharmacol 81, 177–185 [PubMed: 12710532]

17. Tilan JU, Everhart LM, Abe K, Kuo-Bonde L, Chalothorn D, Kitlinska J, Burnett MS, Epstein SE, Faber JE, and Zukowska Z (2013) Platelet neuropeptide Y is critical for ischemic revascularization in mice. FASEB J

18. Tilan J, and Kitlinska J Neuropeptide Y (NPY) in tumor growth and progression: Lessons learned from pediatric oncology. Neuropeptides 55, 55–66 [PubMed: 26549645]

19. Hansel DE, Eipper BA, and Ronnett GV (2001) Regulation of olfactory neurogenesis by amidated neuropeptides. J Neurosci Res 66, 1–7 [PubMed: 11598996]

20. Sheriff S, Ali M, Yahya A, Haider KH, Balasubramaniam A, and Amlal H (2010) Neuropeptide Y Y5 receptor promotes cell growth through extracellular signal-regulated kinase signaling and cyclic AMP inhibition in a human breast cancer cell line. Mol Cancer Res 8, 604–614 [PubMed: 20332211]

21. Medeiros PJ, Al-Khazraji BK, Novielli NM, Postovit LM, Chambers AF, and Jackson DN (2011) Neuropeptide Y stimulates proliferation and migration in the 4T1 breast cancer cell line. International journal of cancer

22. Kitlinska J (2007) Neuropeptide Y in neural crest-derived tumors: effect on growth and vascularization. Cancer Lett 245, 293–302 [PubMed: 16513255]

23. Lin S, Boey D, and Herzog H (2004) NPY and Y receptors: lessons from transgenic and knockout models. Neuropeptides 38, 189–200 [PubMed: 15337371]

24. Pilobello KT, and Mahal LK (2007) Deciphering the glycocode: the complexity and analytical challenge of glycomics. Curr Opin Chem Biol 11, 300–305 [PubMed: 17500024]

25. Wheatley M, and Hawtin SR (1999) Glycosylation of G-protein-coupled receptors for hormones central to normal reproductive functioning: its occurrence and role. Hum Reprod Update 5, 356–364 [PubMed: 10465525]

26. Larhammar D, and Salaneck E (2004) Molecular evolution of NPY receptor subtypes. Neuropeptides 38, 141–151 [PubMed: 15337367]

27. Bischoff A, Puttmann K, Kotting A, Moser C, Buschauer A, and Michel MC (2001) Limited signal transduction repertoire of human Y(5) neuropeptide Y receptors expressed in HEC-1B cells. Peptides 22, 387–394 [PubMed: 11287093]

28. Noda M, Higashida H, Aoki S, and Wada K (2004) Multiple signal transduction pathways mediated by 5-HT receptors. Mol Neurobiol 29, 31–39 [PubMed: 15034221]

29. Pons J, Kitlinska J, Jacques D, Perreault C, Nader M, Everhart L, Zhang Y, and Zukowska Z (2008) Interactions of multiple signaling pathways in neuropeptide Y-mediated bimodal vascular smooth muscle cell growth. Can J Physiol Pharmacol 86, 438–448 [PubMed: 18641693]

30. Czarnecka M, Trinh E, Lu C, Kuan-Celarier A, Galli S, Hong SH, Tilan JU, Talisman N, Izycka-Swieszewska E, Tsuei J, Yang C, Martin S, Horton M, Christian D, Everhart L, Maheswaran I, and Kitlinska J (2015) Neuropeptide Y receptor Y5 as an inducible pro-survival factor in neuroblastoma: implications for tumor chemoresistance. Oncogene 34, 3131–3143 [PubMed: 25132261]

31. Kitlinska J, Abe K, Kuo L, Pons J, Yu M, Li L, Tilan J, Everhart L, Lee EW, Zukowska Z, and Toretsky JA (2005) Differential effects of neuropeptide Y on the growth and vascularization of neural crest-derived tumors. Cancer research 65, 1719–1728 [PubMed: 15753367]

32. Lu C, Everhart L, Tilan J, Kuo L, Sun CC, Munivenkatappa RB, Jonsson-Rylander AC, Sun J, Kuan-Celarier A, Li L, Abe K, Zukowska Z, Toretsky JA, and Kitlinska J (2010) Neuropeptide Y and its Y2 receptor: potential targets in neuroblastoma therapy. Oncogene

33. Nie M, and Selbie LA (1998) Neuropeptide Y Y1 and Y2 receptor-mediated stimulation of mitogen-activated protein kinase activity. Regul Pept 75–76, 207–213

34. Nguyen AD, Mitchell NF, Lin S, Macia L, Yulyaningsih E, Baldock PA, Enriquez RF, Zhang L, Shi YC, Zolotukhin S, Herzog H, and Sainsbury A (2012) Y1 and Y5 receptors are both required for the regulation of food intake and energy homeostasis in mice. PLoS One 7, e40191 [PubMed: 22768253]

35. Herzog H, Darby K, Ball H, Hort Y, Beck-Sickinger A, and Shine J (1997) Overlapping gene structure of the human neuropeptide Y receptor subtypes Y1 and Y5 suggests coordinate transcriptional regulation. Genomics 41, 315–319 [PubMed: 9169127]

36. Wolak ML, DeJoseph MR, Cator AD, Mokashi AS, Brownfield MS, and Urban JH (2003) Comparative distribution of neuropeptide Y Y1 and Y5 receptors in the rat brain by using immunohistochemistry. J Comp Neurol 464, 285–311 [PubMed: 12900925]

37. Movafagh S, Hobson JP, Spiegel S, Kleinman HK, and Zukowska Z (2006) Neuropeptide Y induces migration, proliferation, and tube formation of endothelial cells bimodally via Y1, Y2, and Y5 receptors. Faseb J 20, 1924–1926 [PubMed: 16891622]

38. Kitlinska J, Lee EW, Movafagh S, Pons J, and Zukowska Z (2002) Neuropeptide Y-induced angiogenesis in aging. Peptides 23, 71–77 [PubMed: 11814620]

39. Berglund MM, Schober DA, Esterman MA, and Gehlert DR (2003) Neuropeptide Y Y4 receptor homodimers dissociate upon agonist stimulation. J Pharmacol Exp Ther 307, 1120–1126 [PubMed: 14551289]

40. Dinger MC, Bader JE, Kobor AD, Kretzschmar AK, and Beck-Sickinger AG (2003) Homodimerization of neuropeptide y receptors investigated by fluorescence resonance energy transfer in living cells. The Journal of biological chemistry 278, 10562–10571 [PubMed: 12524448]

41. Gehlert DR, Schober DA, Morin M, and Berglund MM (2007) Co-expression of neuropeptide Y Y1 and Y5 receptors results in heterodimerization and altered functional properties. Biochem Pharmacol 74, 1652–1664 [PubMed: 17897631]

42. Estes AM, McAllen K, Parker MS, Sah R, Sweatman T, Park EA, Balasubramaniam A, Sallee FR, Walker MW, and Parker SL (2010) Maintenance of Y receptor dimers in epithelial cells depends on interaction with G-protein heterotrimers. Amino Acids 40, 371–380 [PubMed: 20577889]

43. Parker MS, Sah R, Balasubramaniam A, Park EA, Sallee FR, and Parker SL (2014) Dimers of G-protein coupled receptors as versatile storage and response units. Int J Mol Sci 15, 4856–4877 [PubMed: 24651459]

44. Parker SL, Parker MS, Estes AM, Wong YY, Sah R, Sweatman T, Park EA, Balasubramaniam A, and Sallee FR (2008) The neuropeptide Y (NPY) Y2 receptors are largely dimeric in the kidney, but monomeric in the forebrain. J Recept Signal Transduct Res 28, 245–263 [PubMed: 18569526]

45. Parker SL, Parker MS, Sah R, Balasubramaniam A, and Sallee FR (2008) Pertussis toxin induces parallel loss of neuropeptide Y Y1 receptor dimers and Gi alpha subunit function in CHO cells. European journal of pharmacology 579, 13–25 [PubMed: 17967449]

46. Parker SL, Parker MS, Sallee FR, and Balasubramaniam A (2007) Oligomerization of neuropeptide Y (NPY) Y2 receptors in CHO cells depends on functional pertussis toxin-sensitive G-proteins. Regul Pept 144, 72–81 [PubMed: 17651824]

47. Kilpatrick LE, Humphrys LJ, and Holliday ND (2015) A G protein-coupled receptor dimer imaging assay reveals selectively modified pharmacology of neuropeptide Y Y1/Y5 receptor heterodimers. Molecular pharmacology 87, 718–732 [PubMed: 25637604]

48. Keller M, Teng S, Bernhardt G, and Buschauer A (2009) Bivalent argininamide-type neuropeptide y y(1) antagonists do not support the hypothesis of receptor dimerisation. ChemMedChem 4, 1733–1745 [PubMed: 19672917]

49. Uegaki K, Murase S, Nemoto N, Kobayashi Y, Yoshikawa S, and Yumoto N (1997) Effects of covalent dimerization on the structure and function of the carboxy-terminal fragment of neuropeptide Y. Biochem Biophys Res Commun 241, 737–743 [PubMed: 9434778]

50. Pfeiffer M, Koch T, Schroder H, Klutzny M, Kirscht S, Kreienkamp HJ, Hollt V, and Schulz S (2001) Homo- and heterodimerization of somatostatin receptor subtypes. Inactivation of sst(3) receptor function by heterodimerization with sst(2A). The Journal of biological chemistry 276, 14027–14036 [PubMed: 11134004]

51. Sorensen G, Lindberg C, Wortwein G, Bolwig TG, and Woldbye DP (2004) Differential roles for neuropeptide Y Y1 and Y5 receptors in anxiety and sedation. J Neurosci Res 77, 723–729 [PubMed: 15352219]

52. Migita K, Loewy AD, Ramabhadran TV, Krause JE, and Waters SM (2001) Immunohistochemical localization of the neuropeptide Y Y1 receptor in rat central nervous system. Brain Res 889, 23–37 [PubMed: 11166683]

53. Tilan JU, Lu C, Galli S, Izycka-Swieszewska E, Earnest JP, Shabbir A, Everhart LM, Wang S, Martin S, Horton M, Mahajan A, Christian D, O'Neill A, Wang H, Zhuang T, Czarnecka M, Johnson MD, Toretsky JA, and Kitlinska J (2013) Hypoxia shifts activity of neuropeptide Y in Ewing sarcoma from growth-inhibitory to growth-promoting effects. Oncotarget 4, 2487–2501 [PubMed: 24318733]

54. Hancock JD, and Lessnick SL (2008) A transcriptional profiling meta-analysis reveals a core EWS-FLI gene expression signature. Cell cycle (Georgetown, Tex 7, 250–256

55. Lu C, Tilan JU, Everhart L, Czarnecka M, Soldin SJ, Mendu DR, Jeha D, Hanafy J, Lee CK, Sun J, Izycka-Swieszewska E, Toretsky JA, and Kitlinska J (2011) Dipeptidyl Peptidases as Survival Factors in Ewing Sarcoma Family of Tumors: IMPLICATIONS FOR TUMOR BIOLOGY AND THERAPY. The Journal of biological chemistry 286, 27494–27505 [PubMed: 21680731]

56. El-Salhy M, and Hausken T (2016) The role of the neuropeptide Y (NPY) family in the pathophysiology of inflammatory bowel disease (IBD). Neuropeptides 55, 137–144 [PubMed: 26431932]

57. Sabban EL, Alaluf LG, and Serova LI (2016) Potential of neuropeptide Y for preventing or treating post-traumatic stress disorder. Neuropeptides 56, 19–24 [PubMed: 26617395]

Highlights

- NPY receptors form homodimers and heterodimers

- Co-expression of heterotypic NPY receptors enables their reciprocal transactivation

- Receptor transactivation can occur independently of heterodimer formation

- Heterotypic NPY receptor interactions increase cell sensitivity to its low levels

- Targeting multiple NPY receptors may improve therapies exploiting NPY system
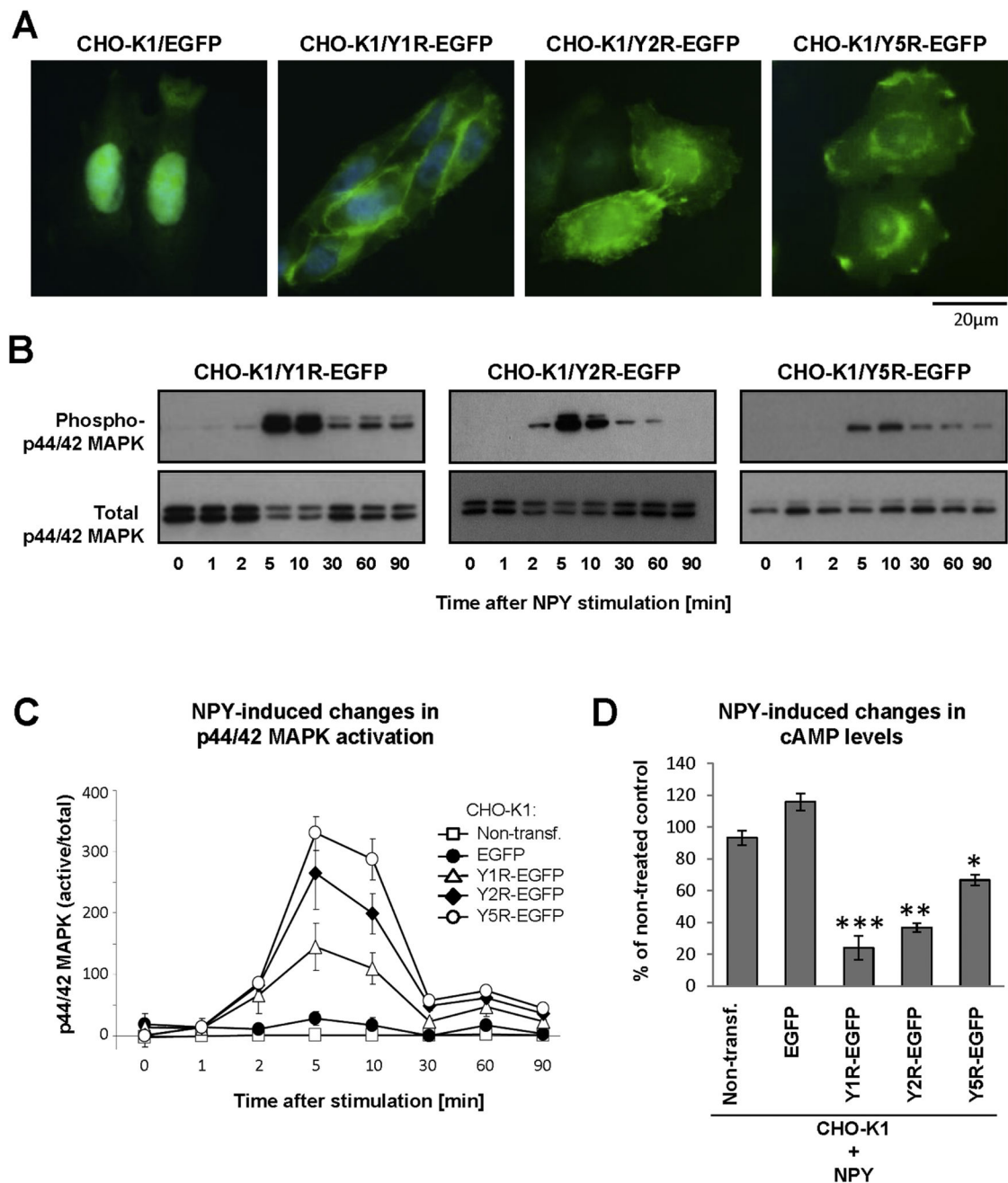
Figure 1. NPY receptors fused to fluorescent proteins preserve their functions.
A. Microscopic images of CHO-K1 cells stably transfected with EGFP alone or NPY receptors fused to EGFP. B. p44/42 MAPK activation induced by NPY in CHO-K1 cells stably transfected with its receptors fused to EGFP. The cells were treated with NPY at a concentration of 10^{-7}M, and phosphorylated and total p44/42 MAPK were detected by Western blot. C. Densitometric quantification of p44/42 MAPK activation in NPY-treated CHO-K1 cells stably transfected with NPY receptor-EGFP fusion proteins. D. NPY-induced changes in cAMP levels in CHO-K1 cells expressing NPY receptors fused to EGFP. The cells were treated with forskolin in the presence or absence of NPY at a concentration of

10^{-7}M for 1h, and the cAMP levels were measured by enzyme immunoassay. The graph represents an average of three independent experiments, 2 wells per treatment each. * p<0.05, ** p<0.01 and ***p<0.001 vs. NPY-treated nontransfected control by t-test.
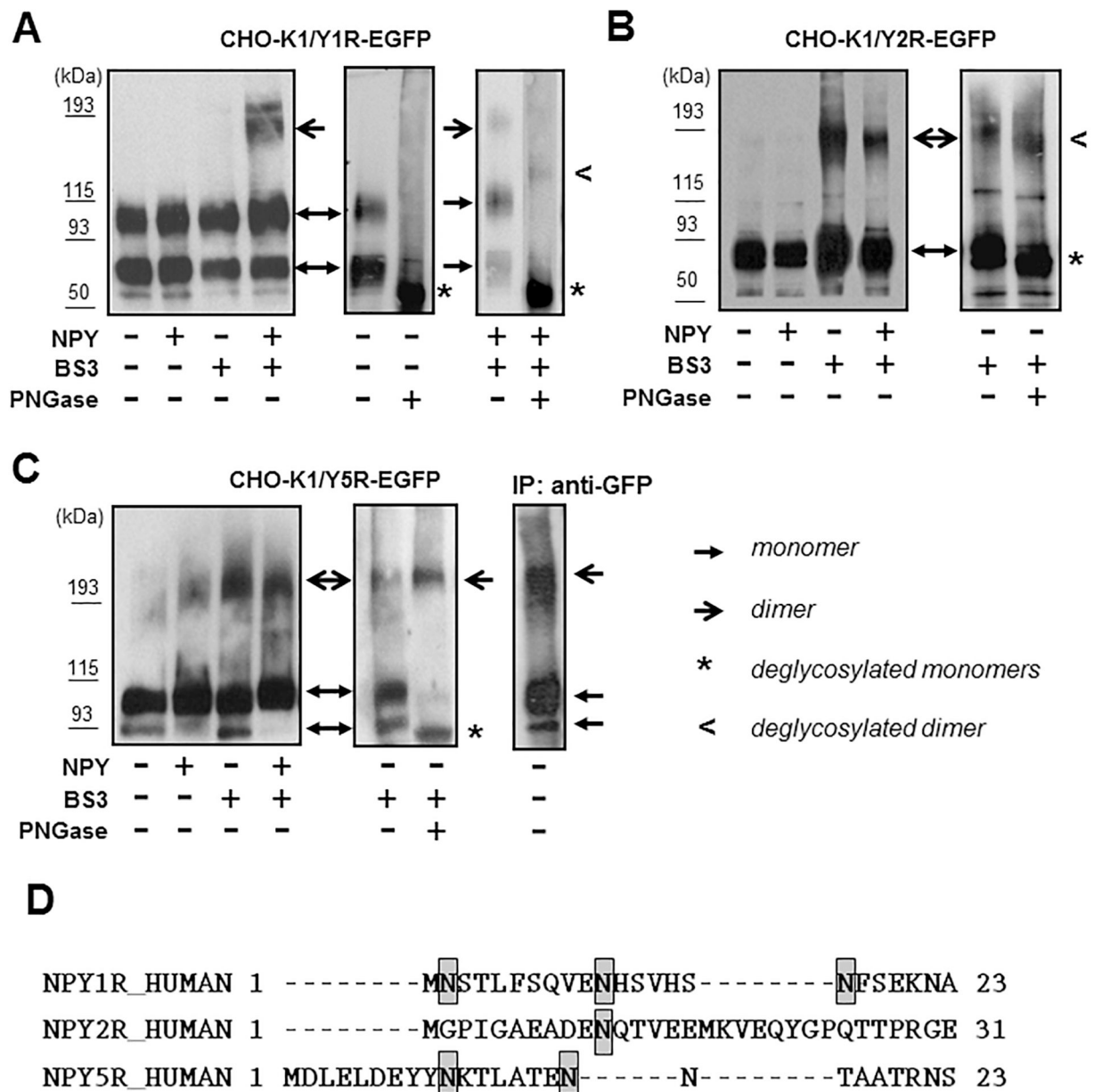
Figure 2. NPY receptors are glycosylated and form homodimers.
A. Western blot analysis of Y1R forms present in membrane preparations from CHO-K1/Y1R-EGFP cells. The cells were treated with NPY at a concentration of 10^{-7}M for 15 min, followed by 30 min incubation with 0.5 mM membrane-impermeable cross-linker, BS3. Y1R-EGPF fusion proteins were detected by Western blot with anti-EGFP antibody (left panel). Membrane preparations from untreated and NPY/BS3-treated CHO-K1/Y1R-EGFP cells were subsequently deglycosylated with PNGase F and subjected to Western blot analysis, as above (right panels). B. Y2R forms in CHO-K1/Y2REGFP cells analyzed by Western blot, as above. Deglycosylation was performed on membrane preparations from cells treated with BS3 cross-linker. C. Y5R forms in CHO-K1/Y5R-EGFP cells analyzed as

above. Additionally, membrane preparation from untreated Y5R transfectants was subjected to immunoprecipitation with anti-EGFP antibody and the Y5R-EGFP forms detected by Western blot (right panel). Each experiment in panels A-C was repeated three times and the representative Western blot results are shown. D. Putative glycosylation sites within N-termini of NPY receptors, based on UniProt analysis.
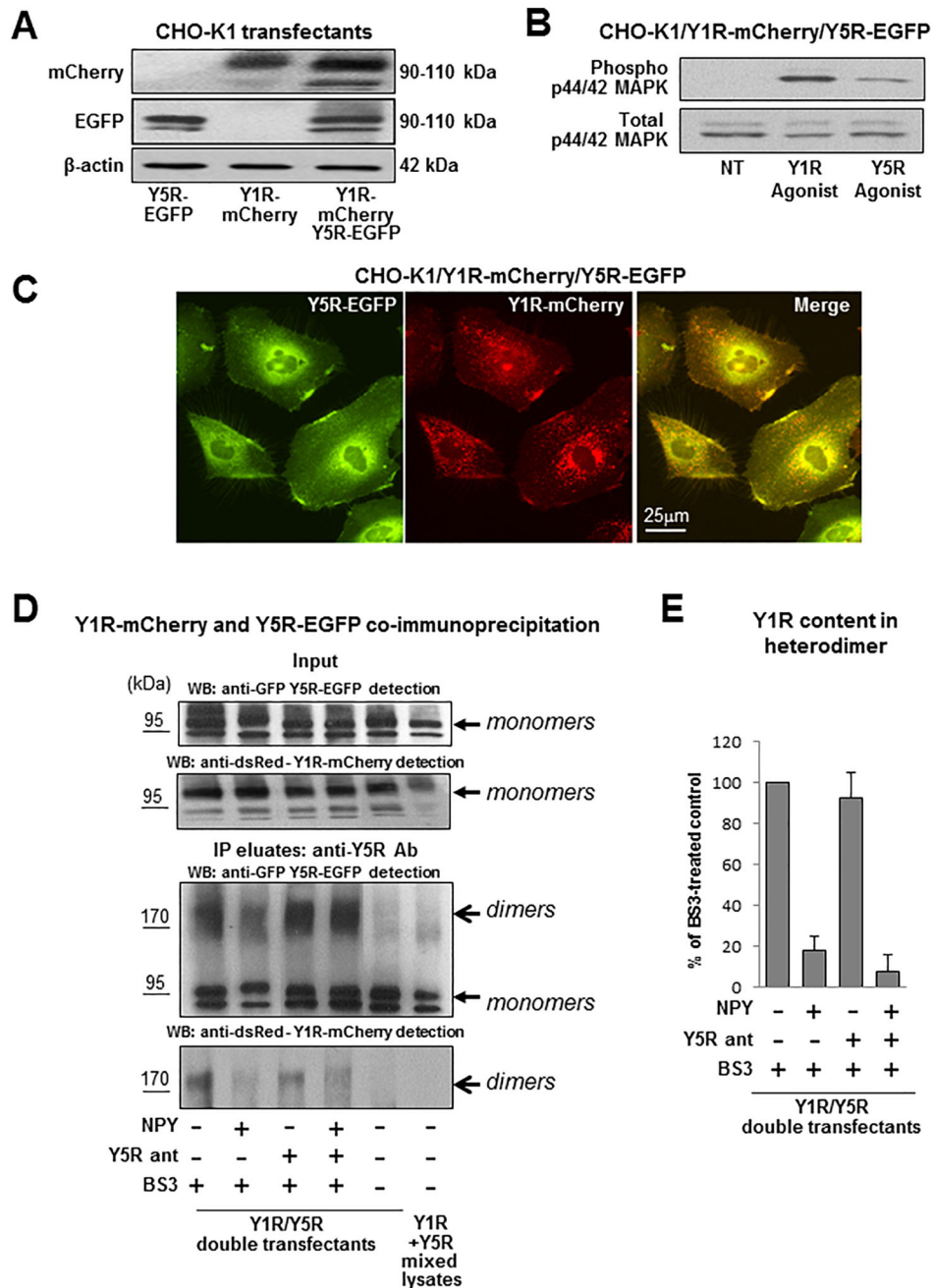
Figure 3. Y1R and Y5R form heterodimers upon co-expression in CHO-K1 cells.
A. Expression of Y1R-mCherry and Y5R-EGFP in CHO-K1 cells transfected with both constructs, detected by Western blot with anti-dsRed and anti-GFP antibody, respectively. B. p44/42 MAPK activation in response to treatment with Y1R- and Y5R-selective agonists ([Arg6, Pro34]NPY and BWX 46, respectively) administered for 5 min at a concentration of 10^{-7}M. C. Fluorescence microscopy of CHO-K1 cells expressing Y1R-mCherry and Y5R-EGFP proteins. D. Western blot analysis of Y1R and Y5R forms in CHO-K1/Y1R-mCherry/Y5R-EGFP cells. The cells were treated with 10^{-7}M NPY for 15 min, with or without 15 min pre-treatment with Y5R antagonist, CGP71683, at a concentration of 10^{-6}M. The cells

were subsequently treated for 30 min with 0.5 mM membrane-impermeable cross-linker, BS3, lysed and subjected to immunoprecipitation with anti-Y5R antibody. The Y1R-mCherry and Y5R-EGFP forms were detected by Western blot with anti-dsRed and anti-EGFP antibody, respectively. The experiment was repeated three times and the representative results are shown. E. Densitometric analysis of the NPY-induced changes in Y1R-mCherry receptor content in the surface heterodimer fraction (>170 kDa band).
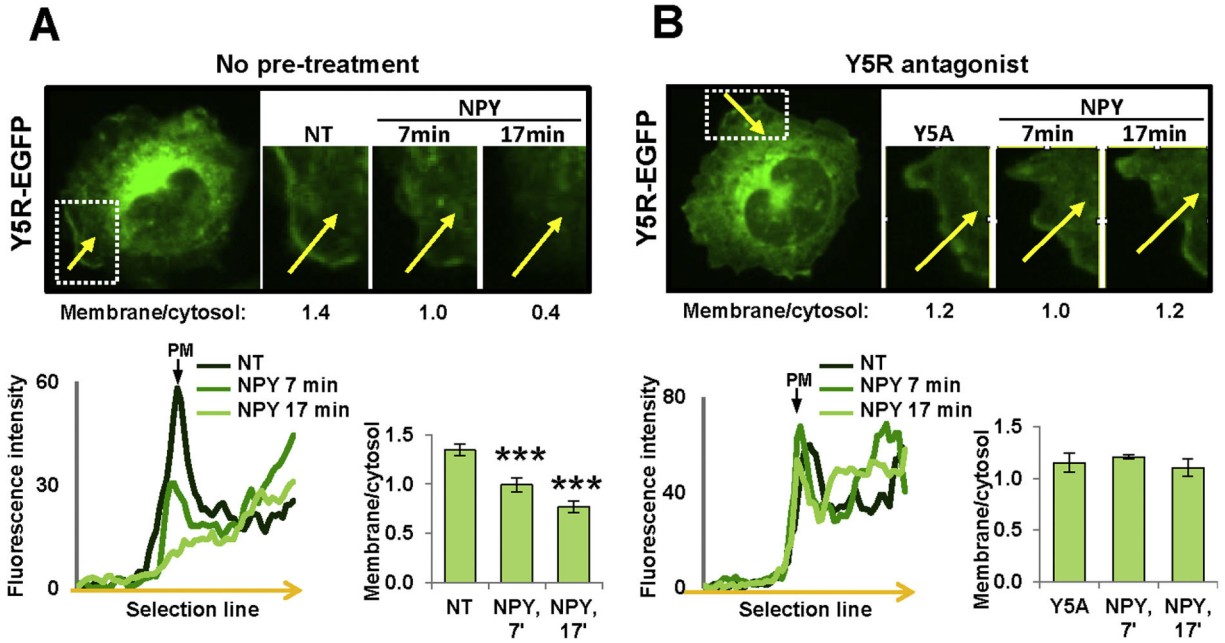
Figure 4. Y5R antagonist blocks NPY-induced Y5R-EGFP internalization.
A. A representative time-lapse fluorescence microscopy image of a cell transfected with
Y5R-EGFP alone, with the marked region of membrane localization of the receptor that was
subjected to analysis (white box). For this region, NPY-induced changes in receptor
localization were measured by comparing ratios of fluorescence at the membrane to the
corresponding sub-membrane cytosol region (membrane/cytosol) before and after treatment,
as indicated by the numbers under the representative images. The linear graph represents the
fluorescence densities across the cell membrane (along the yellow arrow) measured at the
selected region at three time points. The bar graph depicts average membrane/cytosol ratios
at the selected time points upon NPY treatment for all cells analyzed (11 independent
regions). B. Analysis of Y5R-EGFP internalization upon treatment with 10^{-7}M NPY in the
presence of Y5R antagonist, CGP71683, at a concentration of 10^{-6}M. The measurements
and analyses were performed for 5 independent regions, as described for panel A. NT – non-
treated cells; Y5A – cells upon Y5R antagonist pre-treatment; PM – plasma membrane. ***
p<0.001 vs. NT by paired t-test.
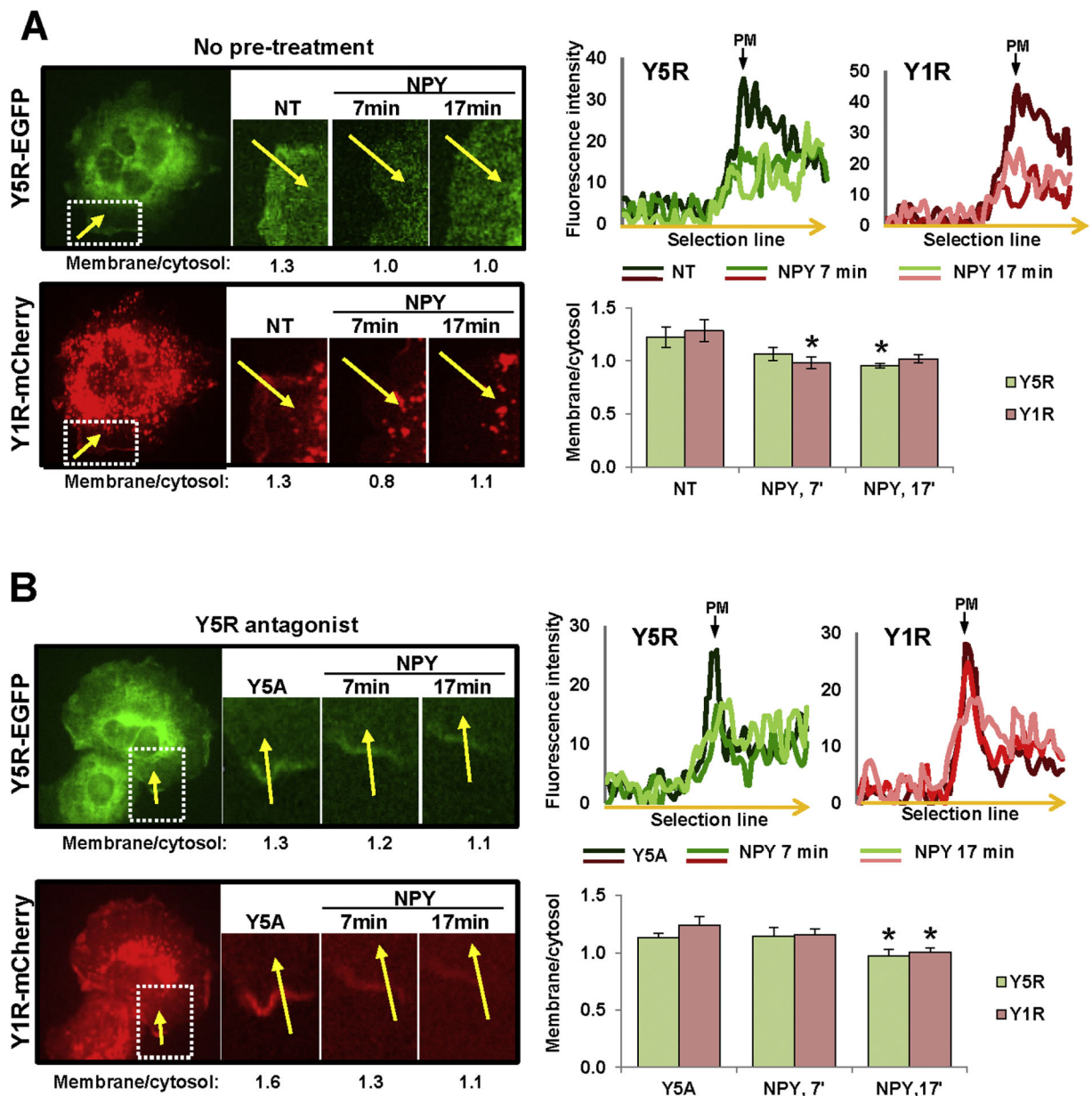
Figure 5. Y5R antagonist does not block NPY-induced internalization of Y5R in CHOK1/Y1R-mCherry/Y5R-EGFP cells.

A. Representative time-lapse fluorescence microscopy images of CHO-K1 cell transfected with Y5R-EGFP and Y1R-mCherry. The region with membrane localization of both receptors was selected for analysis (white box). The numbers below microscopic images indicate fluorescence ratios of the selected membrane section to its corresponding sub-cellular cytosol area (membrane/cytosol) for this representative region at the desired time points upon stimulation with 10^{-7}M NPY. The linear graphs show green and red fluorescence intensities across the membrane in the selected region (along the yellow arrow) at the desired time points upon NPY stimulation. The bar graph depicts quantitative analysis of the membrane/cytosol fluorescence ratios at the selected time points upon NPY

stimulation for all cells analyzed (9 independent regions). B. Analysis of the NPY-induced receptor internalization performed in CHO-K1/Y1R-mCherry/Y5R-EGFP cells pre-treated for 15 min with Y5R antagonist, CGP71683, at a concentration of 10^{-6}M. The cell treatment, measurements and analyses were performed for 7 independent regions, as described above (A). NT – non-treated cells; Y5A – cells upon Y5R antagonist pre-treatment; PM – plasma membrane. * p<0.05 vs. NT by paired t-test.
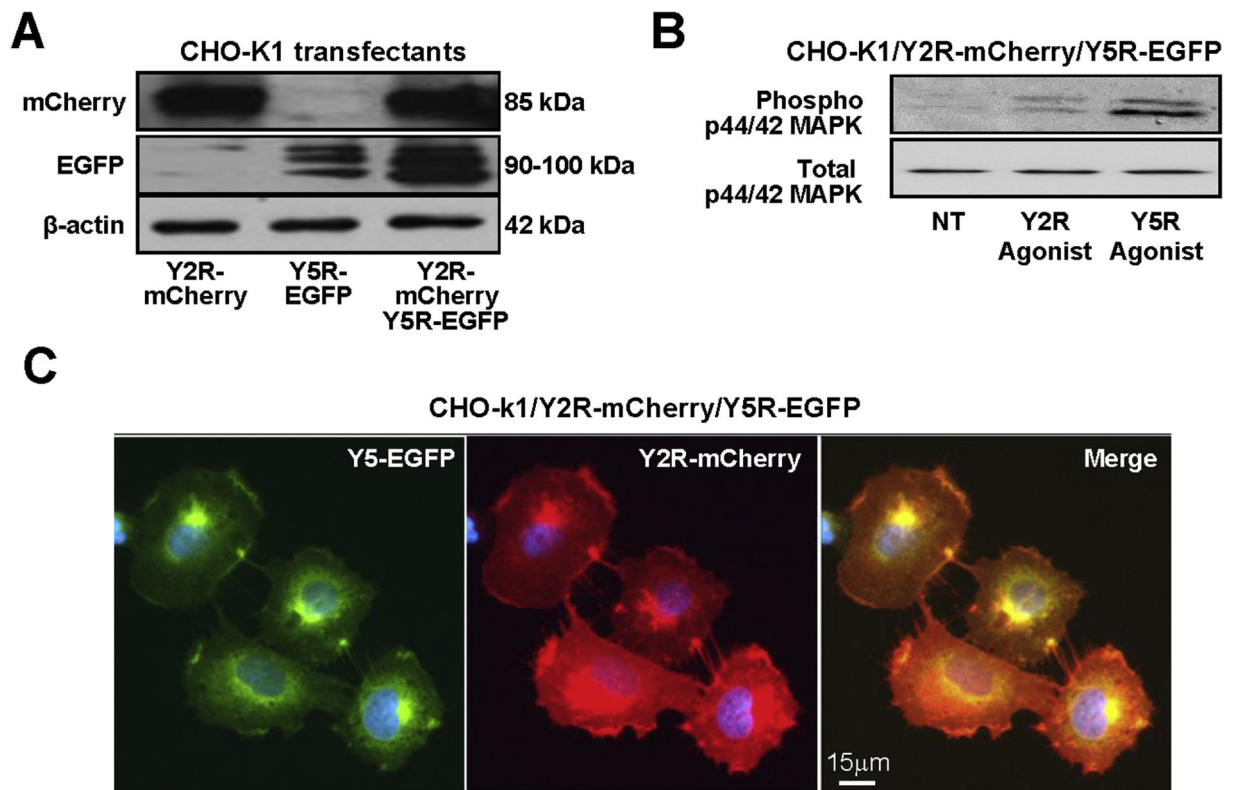
Figure 6. Y2R and Y5R co-localize in CHO-K1/Y2R-mCherry/Y5R-EGFP cells.
A. Expression of Y2R-mCherry and Y5R-EGFP in CHO-K1 cells transfected with both constructs, detected by Western blot with anti-dsRed and anti-EGFP antibody, respectively. B. p44/42 MAPK activation in response to treatment with Y2R- and Y5R-selective agonists ([ahx(5-24)]NPY and BWX 46, respectively) administered for 5 min at a concentration of 10^{-7}M. C. Fluorescence microscopy images of CHO-K1 cells expressing Y2R-mCherry and Y5R-EGFP proteins.
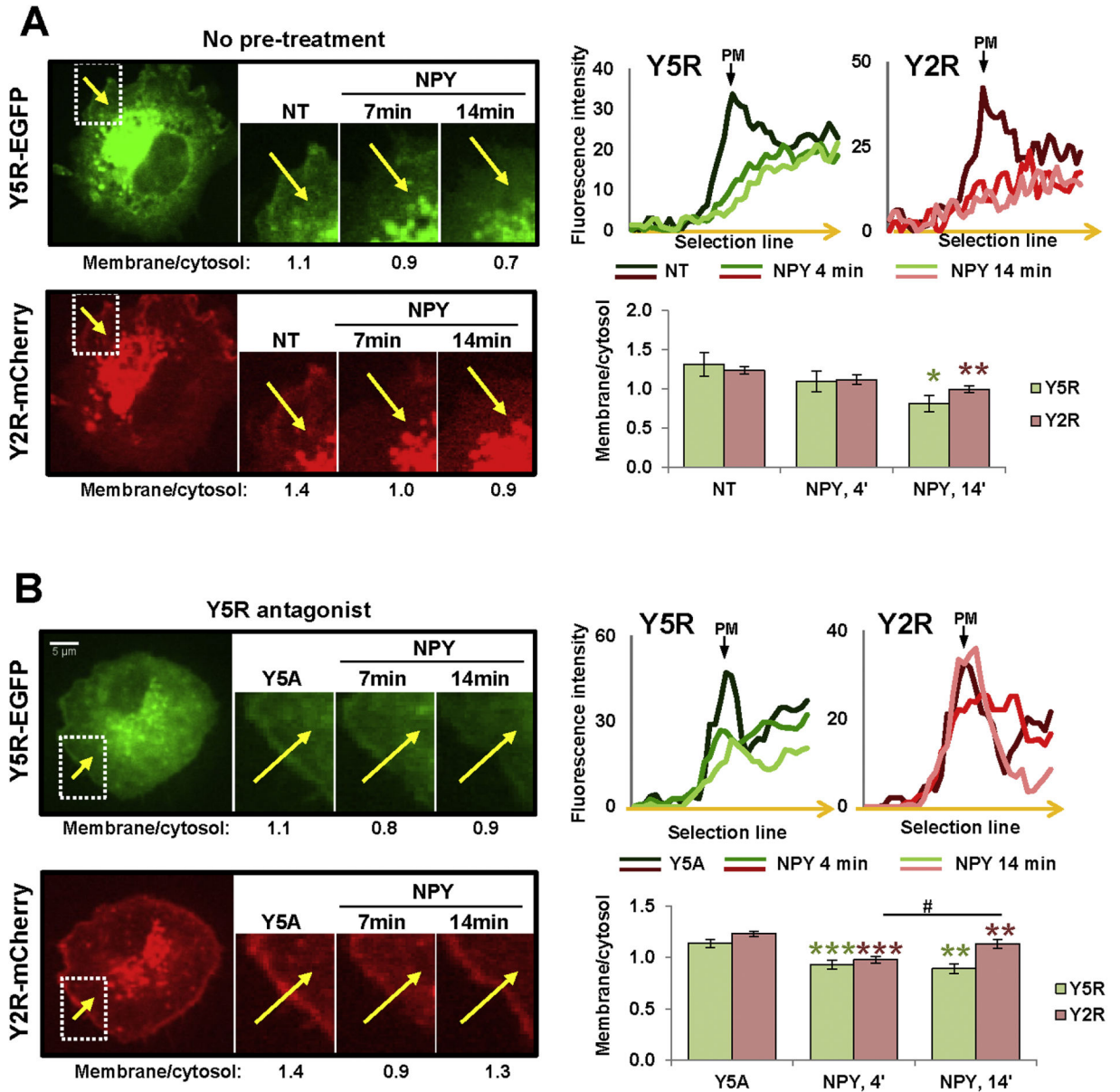
Figure 7. In CHO-K1/Y2R-mCherry/Y5R-EGFP cells, Y5R antagonist does not block NPY-induced internalization of Y5R, yet the recycling rates vary between Y2R and Y5R.

A. Representative time-lapse fluorescence microscopy images of CHO-K1 cell transfected with Y5R-EGFP and Y2R-mCherry. The region with membrane localization of both receptors was selected for analysis (white box). The numbers below microscopic images indicate fluorescence ratios of the selected membrane section to its corresponding sub-cellular cytosol area (membrane/cytosol) for this representative region at the desired time points upon stimulation with 10^{-7}M NPY. The linear graphs show green and red fluorescence intensities across the membrane in the selected region (along the yellow arrow) at the desired time points upon NPY stimulation. The bar graph depicts results of the quantitative analysis of membrane/cytosol fluorescence ratios at the selected time points

upon NPY stimulation for all cells analyzed (16 independent regions). B. Analysis of the NPY-induced receptor internalization performed in CHO-K1/Y2R-mCherry/Y5R-EGFP cells pre-treated with Y5R antagonist, CGP71683, at a concentration of 10^{-6}M. The cell treatment, measurements and analyses were performed for 7 independent regions, as described above (A). NT – non-treated cells; Y5A – cells upon Y5R antagonist pre-treatment; PM – plasma membrane. * $p<0.05$; ** $p<0.01$; *** $p<0.001$ vs. NT; # $p<0.05$, as indicated. The statistical significance was assessed by paired t-test.
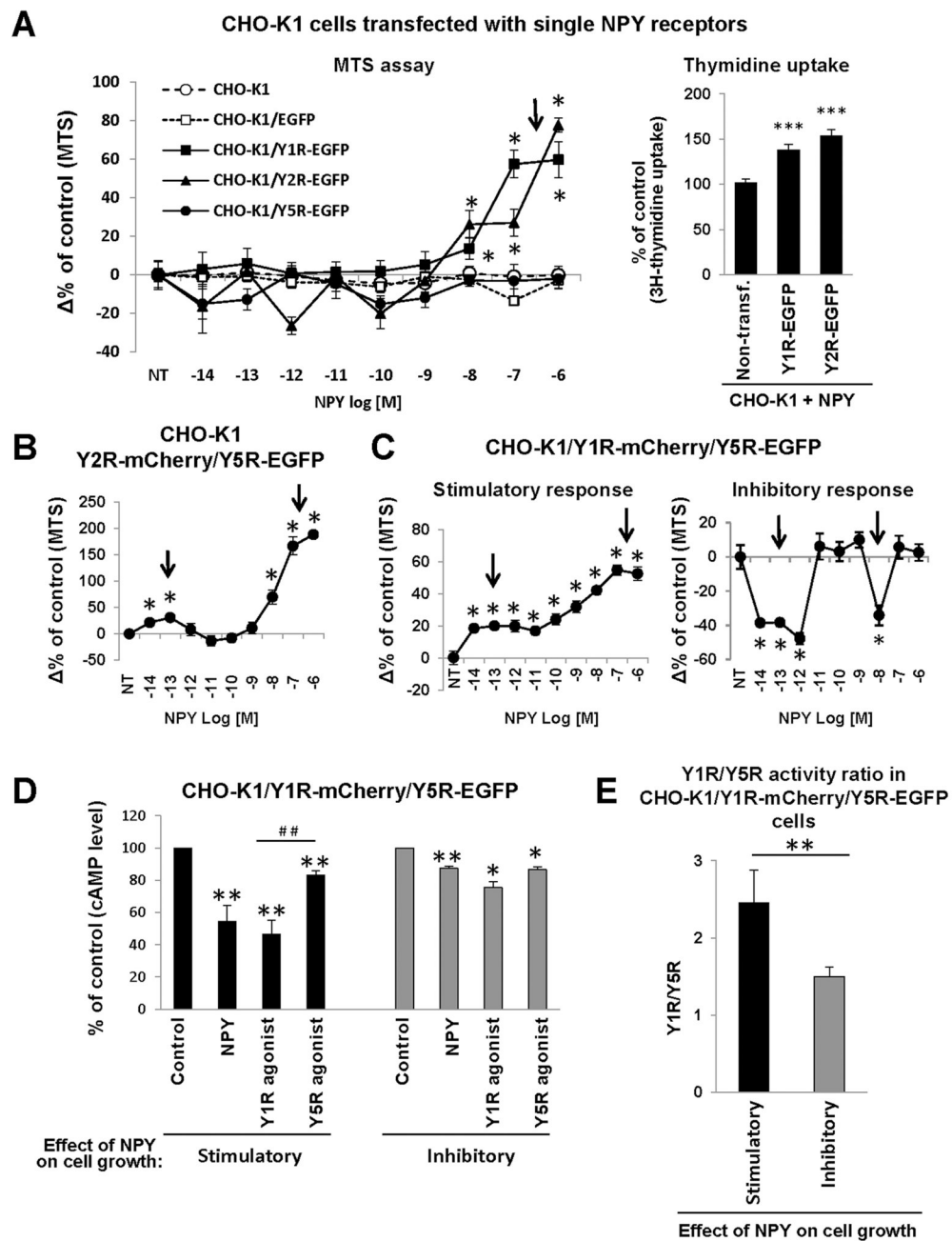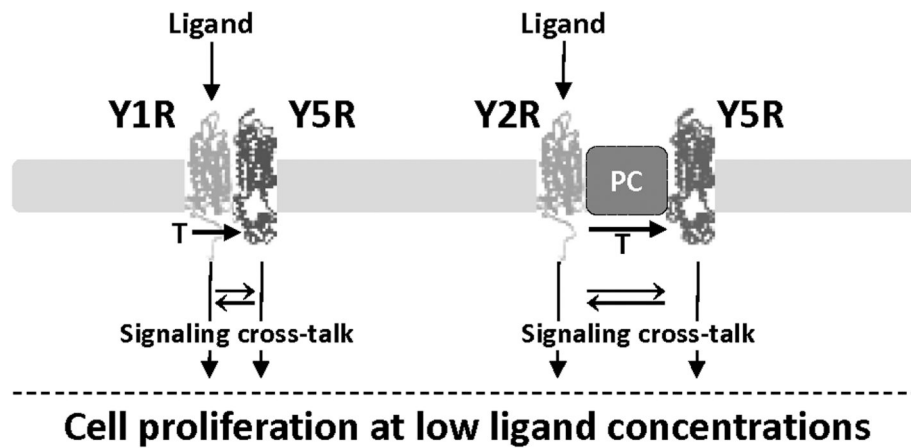
Figure 8. Co-expression of heterotypic NPY receptors enhances its mitogenic effect at picomolar concentrations.

A. Effect of NPY on the number of viable CHO-K1 cells transfected with single NPY receptors and their proliferation, as measured by MTS assay and thymidine uptake, respectively. For thymidine uptake, the cells were treated with 10^{-6}M NPY. B. Changes in the number of viable CHO-K1 cells transfected with both Y2R-mCherry and Y5R-EGFP in response to low and high concentrations of NPY. C. The differential growth response to NPY in CHO-K1/Y1R-mCherry/Y5R-EGFP clones. The number of viable cells in panels B-C was measured by MTS assay. In all experiments above (A-C), cells were treated with NPY

for 24h. NT – non-treated cells; * p<0.05 vs. NT by one way ANOVA followed by Dunnett's test. The experiments were performed 3 times, 6 wells per treatment each, on 2–13 independent transfectant clones per receptor type. The graphs represent average changes in the number of viable cells from all experiments and clones tested. D. Decrease in cAMP levels induced by NPY or selective Y1R or Y5R agonists in CHO-K1/Y1R-mCherry/Y5R-EGFP transfectants with the growth-stimulatory or inhibitory response to NPY. The cells were treated with forskolin in the presence or absence of the desired ligand at a concentration of 10^{-7}M for 1h, and the cAMP levels were measured by enzyme immunoassay. * p<0.05 and ** p<0.01 vs. non-treated control or [##] p<0.01 for Y1R agonist vs Y5R agonist by paired t-test. E. Ratio of Y1R to Y5R activity, as measured by decreased cAMP levels induced by selective Y1R or Y5R agonists, as described in panel D above, and compared in CHO-K1/Y1R-mCherry/Y5R-EGFP with the growth-stimulatory or inhibitory responses to NPY. ** p<0.01 by t-test. The experiments in panels D-E were performed 3 times, 2 wells per treatment each, on 5 and 3 CHO-K1/Y1R-mCherry/Y5REGFP clones with the growth-stimulatory or inhibitory response to NPY, respectively. The graphs represent average changes in cAMP levels from all experiments and clones tested.

Figure 9. Model of the mechanisms underlying increased ligand sensitivity in cells expressing heterotypic NPY receptors.
Y1R and Y5R form heterodimers, while Y2R and Y5R are not directly bound, yet interact with each other, possibly as a part of the larger protein complex (PC). However, in either case, activation of one receptor in the complex leads to transactivation (T) of the other NPY receptor and signaling from both receptors. This, in turn, may trigger signaling cross-talk between pathways activated by these receptors and thereby enhance their functional effects. Consequently, cells expressing heterotypic NPY receptors proliferate in response to low ligand concentrations.